Induction Machine Diagnosis using Stator Current Advanced Signal Processing

Elhoussin Elbouchikhi[1], Vincent Choqueuse[2] and Mohamed Benbouzid[2,3]

Abstract – *Induction machines are widely used in industrial applications. Safety, reliability, efficiency and performance are major concerns that direct the research activities in the field of electrical machines. Even though the induction machines are very reliable, many failures can occur such as bearing faults, air-gap eccentricity and broken rotor bars. Therefore, the challenge is to detect them at an early stage in order to prevent breakdowns. In particular, stator current-based condition monitoring is an extensively investigated field for cost and maintenance savings. In fact, several signal processing techniques for stator current-based induction machine faults detection have been studied. These techniques can be classified into: spectral analysis approaches, demodulation techniques and time-frequency representations. In addition, for diagnostic purposes, more sophisticated techniques are required in order to determine the faulty components. This paper intends to review the spectral analysis techniques and time-frequency representations. These techniques are demonstrated on experimental data issued from a test bed equipped with a 0.75 kW induction machine.*

Keywords*: Induction machines, condition based maintenance, faults detection, signal processing, spectral analysis.*

Nomenclature

O&M = Operation and Maintenance;
WTG = Wind Turbine Generator;
MMF = Magneto-Motive Force;
MCSA = Motor Current signal Analysis;
PSD = Power Spectral Density;
FFT = Fast Fourier Transform;
DFT = Discrete Fourier Transform;
MUSIC = MUltiple SIgnal Characterization;
ESPRIT = Estimation of Signal Parameters via Rotational Invariance Techniques;
SNR = Signal to Noise Ratio;
MLE = Maximum Likelihood Estimation;
STFT = Short-Time Fourier Transform;
CWT = Continuous Wavelet Transform;
WVD = Wigner-Ville distribution;
HHT = Hilbert-Huang Transform;
DWT = Discrete Wavelet Transform;
EMD = Empirical Mode Decomposition;
IMF = Intrinsic Mode Function;
AM = Amplitude Modulation;
FM = Frequency Modulation;
IA = Instantaneous Amplitude;
IF = Instantaneous Frequency;
f_s = Supply frequency;
f_r = Rotational frequency;
f_c = Fault frequency introduced by the modified rotor MMF;
f_d = Characteristic vibration frequencies;
f_{bng} = Bearing defects characteristic frequency;
f_{od} = Bearing outer raceway defect characteristic frequency;
f_{id} = Bearing inner raceway defect characteristic frequency;
f_{bd} = Bearing balls defect characteristic frequency;
f_{ecc} = Eccentricity characteristic frequency;
N_r = Number of rotor bars or rotor slots;
s = Slip;
F_s = Sampling frequency;
N = Number of samples;
$w[.]$ = Time-window (Hanning, Hamming, etc.);
τ = Time-delay;
σ^2 = Variance;
$h[.]$ = Time-window.

I. Introduction

In the field of energy production and many other industrial applications, the electrical drives are subject to various failures, possibly combined. These faults include: failure of power supply devices, failure of electrical machine, failure of mechanical load (wear or breakage of all or part of the bearings, shafts, gears, etc.), failure of control devices, failure of cables, connections, protective devices, etc.

Induction machines are still the most important rotating electric machines in industry mainly because of their low price, ruggedness, efficiency and reliability. Although, the use of switching power converters has improved the performance of such machines and has extended its use to adjustable speed drives, the electrical machine lifetime has been reduced. This fact has increased the range of applications where the need of diagnostics is crucial.

Typical faults in induction machines include: Stator faults; opening or shorting of one or more of a stator phase winding, broken rotor bar or cracked rotor end-rings, static and/or dynamic air-gap irregularities, bent shaft and misalignment, bearing and gearbox failures, failure of one or more power electronic components of the drive system [1].

These failures are due to various causes, which are associated with the design, manufacture or employment processes. These faults can have as consequences: magnetic field distortion, risk of stator damages, overheating phenomena, risks of electric arcs, vibration effects, abnormally high or destructive currents, electromechanical torque oscillation, noise and problem of additional torque. If undetected, these faults may cause catastrophic failures. Consequently, it is mandatory to define a maintenance strategy. In particular, it is suitable to develop a maintenance strategy that meets the requirements of machine availability and operational safety, at minimum cost. Hence, condition based maintenance is the appropriate strategy that meets the reliability and availability requirements.

Most methods for induction machine monitoring could be classified into several categories: vibration monitoring, torque monitoring, temperature monitoring, oil/debris analysis, acoustic emission monitoring, optical fiber monitoring, and current/power monitoring [2-3]. In particular, stator current based condition monitoring is an extensively investigated field for cost and maintenance savings [4-6]. Hence, in this paper attempts are made to highlight induction machine faults effects over the stator current. Moreover, emphasis is made on condition monitoring techniques based on stator current processing which is already measured on the drive system for other purposes such as control and protection.

The remaining parts of the present paper are organized as follows. Section II reports on the condition monitoring techniques used in the industry and presents the induction machine faults effect over the stator currents. Section III summarizes the signal processing techniques commonly used in order to detect a fault and measure its severity. This section focuses on the spectral estimation techniques and the time-frequency representations. Finally, section IV concludes this paper and gives some perspectives for further investigations.

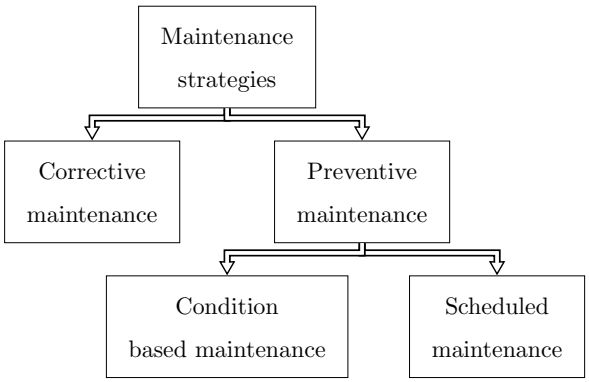

Fig. 1. Classification of maintenance types [7].

II. Condition Monitoring of Induction Machines

Shutdown of plants due to unexpected breakdowns and failures of induction machines are extremely costly in terms of time and money. Therefore, reducing operation and maintenance costs (O&M) is becoming a crucial motivation. Several techniques have been proposed for condition monitoring and faults detection in order to increase the reliability of such systems and therefore reduce the O&M costs.

II.1. Maintenance Strategies

The maintenance is required for almost all types of machines in various industrial applications in order to improve the reliability and decrease operating and maintenance costs. The type of maintenance that is performed can be classified as either corrective or preventive maintenance (see Fig. 1). The corrective maintenance is carried out after a failure and is intended to repair the system. The corrective maintenance presents several drawbacks: risk of catastrophic failures, production loss, and reliability decrease. The preventive maintenance is intended to reduce the probability of failure and include scheduled maintenance and condition based maintenance. The scheduled maintenance is considered as cyclic maintenance strategy which is carried out at predetermined intervals, whereas the condition based maintenance tries to find the optimum time for carrying out the required maintenance actions by monitoring the current state of a specific component. The scheduled maintenance can be either clock-based or age-based maintenance. This means that components exposed to wear of fatigue are replaced regularly even if they are not at the end of their lifetime. Nevertheless, the scheduled maintenance presents a higher cost compared to corrective maintenance.

Consequently, the most interesting preventive maintenance is the condition-based maintenance. The condition-based maintenance offers the possibility to schedule the maintenance activities. Moreover, the components may be used until their full life and defects may be detected at an early stage in order to prevent breakdowns and afterwards reduce downtime and maintenance cost. Even though such techniques require additional condition monitoring hardware and software, the overall maintenance cost is significantly decreased. The challenge concerning the condition-based maintenance is to determine when the maintenance actions must be performed. Monitoring the condition of components in order to be able to plan maintenance actions prior to failure and then minimize downtime and repair costs may do this. This aspect is still under investigation and several methods have been proposed relying on various sensors and different measured quantities.

II.2. Induction Machine Condition Monitoring and Faults Detection Methods

Condition based maintenance of induction machine in industrial applications is based on several parameters monitoring. According to the sensor measurement used, most methods for induction machine monitoring could be classified into several categories: vibration monitoring [8-9], torque monitoring, temperature monitoring, oil/debris analysis, acoustic emission monitoring, optical fiber monitoring, and current/power monitoring [2-3].

Most faults generated in induction machine or associated components cause additional vibrations. A bearing fault, for instance, can generate a radial rotor movement and a shaft torque variation in the induction machine, and consequently vibration of the whole electromechanical drive [8], [10]. Vibration monitoring has been intensively studied in academia and widely used in industrial applications. Therefore, commercial condition monitoring and fault detection system are mostly performed based on vibration monitoring [11]. However, this technique is sophisticated and costly [12]. Moreover, the vibration sensors are mounted on the surface of the electromechanical drives and can be difficult to access during induction machine operation. These sensors are subject to failures, which cause additional maintenance cost and affect the system reliability. For instance, it has been reported that sensor failures contribute to more than 14% of failures in wind turbine systems [13].

It has been demonstrated that most of faults lead to torque oscillations and rotor imbalance [14]. Hence, torque monitoring has been used to detect faults of the induction machine [10]. It has also been applied to detect generator stator windings short-circuit in a WTG [15]. However, the torque transducers need to be installed in the shaft to measure the electrical machine torque, which increase the cost and the complexity of the monitoring system. Temperature measurement is generally performed for bearing faults monitoring. The IEEE standard 841 points out that the stabilized bearing temperature rise at the rated load should not exceed 45°C [16]. Therefore, abrupt temperature increase (for example, the lack of lubrication) means the failure of the bearings. Much like, the temperature of gearbox oil in WTG should be in certain range during wind turbine rated operating conditions. The main drawback of temperature monitoring is that the measured temperature may be affected by multiple factors (environment temperature, stator current heating, and generator rotating speed) [17]. Oil/debris analysis is currently used for condition monitoring in industry [18]. In fact, analyzing the composition, content, size, and classification of wear particles in lubrication oil of bearings and many other components of induction machine allow determining their health conditions. However, this method only works for high power rating electrical machines with oil lubricated bearings. Many other methods exist such as acoustic emission monitoring [19], optical fiber monitoring, flux monitoring [20]. However, these techniques are more complicated in real-world applications and require additional sensors, which increase the price/complexity of the monitoring system.

This survey of condition-based maintenance approaches highlights the need for a non-invasive, lower cost, most effective condition monitoring approach. A promising technique relies on current/power monitoring. It is based on current and/or voltage measurements that are already available for control and protection purposes. Hence, no additional sensors and acquisition devices are required. Moreover, current/voltage signals are reliable and easily accessible. It follows that current/power monitoring is of great economic interest and can be adopted by industry. Hence, several research activities have been focused on current based faults detection in electrical machines [21-24]. Power measurements have also been investigated [25-26]. However, the challenge in using current and/or voltage signals for condition monitoring is to propose signal processing techniques allowing to extract a fault detection and diagnosis criteria in stationary and non-stationary environment (variable speed drives, WTGs, etc.) and intelligent diagnosis scheme able to classify faults and foresee a potential failure.

II.3. Faults Effect over the Stator Current

The induction machine faults lead to various effects on intrinsic parameters and quantities of the electrical machine, which can be classified in three major categories [27]:

- Faults leading to eccentricity between stator and rotor: bearing defects, shaft misalignment and centering defect;
- Failures introducing torque oscillations: mechanical load defect and bearing faults;
- Defects leading to disturbance in magnetomotive forces: stator short circuit defects, broken electrical connections in the stator.

These effects have an impact over the three phase stator currents. Two main contributions could be presented. The first considers the introduction of additional frequencies on the current power spectral density [1], [28]. The second states that the stator currents are phase and/or amplitude modulated due to the presence of a specific fault [14], [27].

II.3.1. Faults related frequencies

A healthy induction machine contains a great number of spectral components due to its supply voltage, rotor slotting and possible iron saturation (see Table I).

In presence of faults, additional frequency components appear on the stator currents spectrum. Several research activities have focused on these faults related frequencies monitoring [29], [30]. In particular, stator faults detection has been widely investigated with special attention to short-circuits [31-32]. Effective fault detection procedure may combine the use of fault detection techniques and the monitoring of turn-to-turn insulation in order to prevent catastrophic failure.

TABLE I
SYNOPSIS OF STATOR CURRENTS FREQUENCY COMPONENTS UNDER HEALTHY CONDITIONS

Stator current harmonics	Frequency	Origin
Fundamental frequency	f_s	Supply voltage
Time harmonics	$n \times f_s$	Supply voltage harmonics PWM inverters
Rotor slot harmonics	$k\,N_r\,f_r \pm n\,f_s$	Modified airgap
Saturation harmonics	$f_s \pm 2\,k\,f_s$	Deformation of flux density
Torque/speed oscillation and eccentricity	$nf_s \pm f_c$ $nf_s \pm f_r$ $nf_s \pm f_r$	Modified rotor MMF Modified airgap Torque oscillation

MCSA has also been investigated for broken rotor bar and end-ring faults detection in induction machine [33-35]. Hence, diagnosis procedure has been proposed that relies on monitoring frequency components at $(1 \pm 2ks)f_s$, where $k \in \mathbb{N}$. For $k \neq 0$, these components are usually called sideband components [36-38].

Mechanical faults detection based on stator currents have been widely investigated. Bearings defects have been typically categorized as distributed or local [39-40]. Local defects cause periodic impulses in vibration signals. Amplitude and frequency of such impulses are determined by shaft rotational speed, fault location, and bearing dimensions (Fig. 2).

Since ball bearings support the rotor, any bearing defect will produce a radial motion between the rotor and the stator of the machine (air-gap eccentricity), which may lead to anomalies in the air-gap flux density. As the stator current for a given phase is linked to flux density, the stator current is affected as well by the bearing defect. In [41-42], it has been demonstrated that the characteristic bearing fault frequencies in vibration can be reflected on stator currents. The relationship between vibration frequencies and current frequencies for bearing faults can be described by (1)

$$f_{bng} = |f_s \pm k f_d| \quad (1)$$

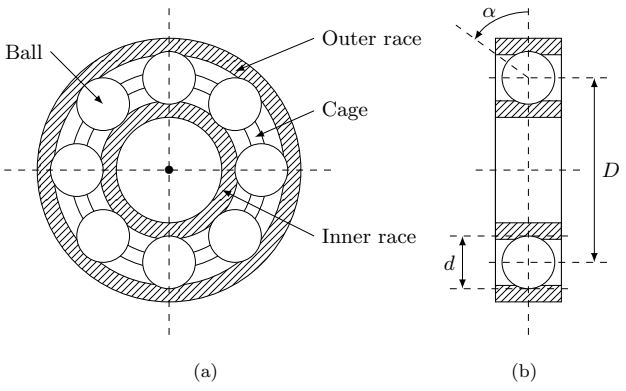

Fig. 2. Bearing structure with main dimensions.

where $k = 1, 2, 3, \ldots$

It is well established that for bearing single-point defects, the characteristic stator current fault frequencies are good fault indicators [42-43]. In fact, by means of (1), it is possible to analyze the specific fault-related frequencies in order to find abnormalities in their amplitude values. There are a large number of papers dealing with the detection and diagnosis of bearing faults based on the stator current of the induction machine [43-46]. Extensive investigations have been conducted on single defects, while generalized roughness (lubrication defects, wear of bearings, etc.) is of great interest. Table II gives a summary of bearing related frequencies in the stator current spectrum.

Eccentricity fault effect has been studied to model the fault impact on stator current [47-49]. It has been proven, that under eccentricity faults, the stator currents contain the frequencies given by (2). It is worth noting that when other mechanical problems such as torque oscillation, these characteristic frequencies may be hidden.

$$f_{ecc} = f_s \left|1 \pm k\left(\frac{1-s}{p}\right)\right| \quad (2)$$

II.3.2. Stator currents modulation

In [14], [43], the authors have presented an analytical approach for the modeling of mechanical and bearing faults based on traditional magnetomotive force (MMF) and permeance wave approach for computation of the airgap magnetic flux density [50]. These studies have demonstrated that mechanical faults may lead to eccentricity and load oscillation faults. The eccentricity fault is responsible of the amplitude modulation of the stator currents and the load oscillation leads to frequency modulation of the stator currents. The modulation frequency depends on the operating conditions of the machine and the fault severity. Moreover, depending on the defective components of the bearings, the stator currents are modulated (amplitude and/or frequency modulation) [51].

In general way, in presence of fault, the current is sinusoidally frequency or amplitude-modulated signal. Based on this signal modeling approach, it seems that the most adapted tool to extract fault indicator is demodulation techniques.

TABLE II
SUMMARY OF BEARING FAULT-RELATED FREQUENCIES: COMPARISON OF TWO STUDIES

Bearing fault	According to [42]	According to [43]	
		Eccentricity	Torque oscillations
Outer raceway	$f_s \pm k\,f_{od}$	$f_s \pm k\,f_{od}$	$f_s \pm k\,f_{od}$
Inner raceway	$f_s \pm k\,f_{id}$	$f_s \pm f_r \pm k\,f_{id}$	$f_s \pm k\,f_{id}$
Ball defects	$f_s \pm k\,f_{bd}$	$f_s \pm f_{cage} \pm k\,f_{bd}$	$f_s \pm k\,f_{bd}$

However, this modeling approach suffers from many restrictive assumptions and lack of generality since it cannot be applied for all type of faults.

II.3.3. Discussion

The two approaches seem to be different. However, we can consider reasonably that the two approaches are equivalent since both of them assume introduction of frequency components in the stator currents due to faults. Moreover, the modulation approach is more restrictive than the first one since it supposes the upper sidebands and lower sidebands have the same amplitude. Furthermore, in the case of phase modulation, the amplitude of sidebands is governed by Bessel functions [27].

III. Stator Current Processing for Induction Machine Faults Features Extraction

In the following, commonly used feature extraction techniques are presented. Specifically, we focus on the stationary techniques and the time-frequency representations. These techniques are demonstrated for bearing faults detection on a 0.75-kW squirrel cage induction machine.

III.1. Stationary Techniques

Techniques presented herein can be classified into two mean categories: the non-parametric techniques (precisely the periodogram and its extensions) and high-resolution techniques.

III.1.1 Periodogram and its extensions

The power spectral density (PSD) $P_x(f)$ of discrete-time process is defined as the Fourier transform of its auto-correlation function [52]. The periodogram is a PSD estimator of a complex discrete-time wide sense stationary random process $x[n]$ and it is defined as follows

$$\hat{P}_x(f) = \frac{1}{N}\left|\sum_{n=0}^{N-1} x[n] e^{\frac{-j2\pi fn}{Fs}}\right|^2 \qquad (3)$$

Hence, the frequency resolution is equal to the inverse of the signal acquisition duration.

The periodogram is usually implemented using the FFT algorithm since it rapidly computes the DFT. It should be noted that the periodogram is biased (the distance between the average of the estimates, and the single parameter being estimated is not zero) and inconsistent estimator (the variance does not decrease to zero when the data record length goes to infinity) of the power spectral density [53]. This can be overcome if several realizations $x_m[n]$ of the same random process $x[n]$ are available. This is performed using Welch periodogram; the signal is split up into overlapping segments, the periodogram of each segment multiplied by a time-window is computed and then averaged. Hence, the Welch periodogram is defined as:

$$\hat{P}_w(f) = \frac{1}{L}\sum_{k=1}^{L} \hat{P}_{xw}^{(k)}(f) \qquad (4)$$

where $\hat{P}_{xw}^{(k)}$ represents the periodogram of the windowed signal $x[n]w[n-\tau k]$.

For illustration purpose, Figs. 3(a), and 3(b) depict the stator current periodogram, and the Welch periodogram, respectively. The periodogram was computed using a signal length of $10s$, a sampling frequency of $1kHz$, and the Hamming window. The Welch method splits the data into eight overlapping segments, each with a 50% overlap, computes the modified periodograms of the overlapping segments, and averages the resulting periodograms to produce the PSD estimate. Each segment is windowed with a Hamming window that is the same length as the segment.

The Welch periodogram enhance estimation performance. Unfortunately, it decreases the spectral precision and resolution due to segmentation. In order to increase the frequency resolution, the signal acquisition time must be increased. Unfortunately, the stationary signal assumption may no longer hold if the signal acquisition time is too long. The periodogram and its extensions are non-parametric methods, i.e. they do not require any a priori knowledge about the signal.

III.1.2 High resolution techniques

If an a priori signal model is assumed, parametric methods can be employed to improve the frequency resolution. In fact, parametric methods can yield higher resolution than non-parametric methods in case where the signal length is short. This is due to their ability to resolve spectral lines separated in frequency by less than $\frac{1}{N}$ cycles per sampling interval, which is the resolution limit for the classical periodogram-based methods [54]. These techniques are generally called high-resolution methods and include three sub-classes: the linear prediction methods, the subspace techniques, and the maximum likelihood estimation. In this paper, we focus on subspace techniques and maximum likelihood estimation.

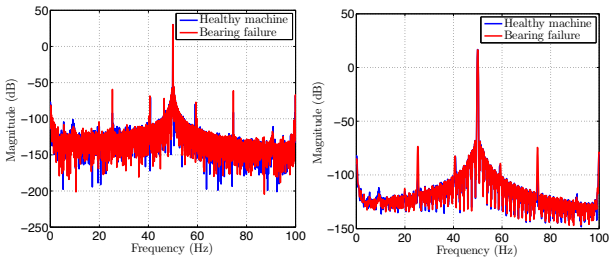

(a) Periodogram. (b) Welch periodogram.

Fig. 3. PSD of stator current with bearing fault vs healthy case.

The subspace class includes the MUSIC and ESPRIT approaches [54]. These techniques are considered as parametric methods for line spectra estimation. These approaches assume the noise to be a white Gaussian noise with zero mean and variance σ^2. These methods relie on singular value decomposition of the samples covariance matrix, which allow separating the signal subspace and the noise subspace.

MUSIC is based on the eigenvalues decomposition of the covariance matrix $\boldsymbol{R_{xx}}$ of measurement data $\boldsymbol{x[n]} = [x[n], x[n+1], \dots, x[n+M-1]]^T$ and the computation of the associated eigenvectors. The summary of the MUSIC algorithm is described in **algorithm (1).** The MUSIC algorithm gives the pseudo-spectrum since it compute the frequency content of signals without calculating their power. To overcome this issue RootMUSIC has been presented. It computes the estimated discrete frequency spectrum, along with the corresponding signal power estimates. Figure 4(a) gives the MUSIC pseudo-spectrum of the stator current. However, although the performance advantages of MUSIC are substantial, they are obtained at a cost in computation (searching over parameter space) and storage. Moreover, its performance depends on the covariance matrix estimator and the SNR.

To reduce computational cost of the spectral estimation, ESPRIT has been proposed. In fact, this technique relies on matrix eigenvalues computation, which allows directly extracting the frequency content, rather than leading to optimization problem like the MUSIC procedure. The ESPRIT method is given by **algorithm (2)**. Figure 4(c) gives the PSD estimation based on ESPRIT. Since the ESPRIT procedure gives only the frequency content, least squares have been used for frequency bins amplitude estimation [52].

Algorithm 1: MUSIC algorithm

Require: Signal samples $\boldsymbol{x}[n]$.

1. Compute the covariance matrix estimate $\widehat{\boldsymbol{R}}_{\boldsymbol{xx}} = \frac{1}{G}\sum_{n=0}^{G-1} \boldsymbol{x}[n]\boldsymbol{x}[n]^H$. Where $(.)^H$ refers to Hermitian matrix transpose. Since $\boldsymbol{x}[n]$ has length M and we have N observations of $x[n]$, we can construct a set of $G = N - M + 1$ different subvectors $\{\boldsymbol{x}[n]\}_{n=0}^{G-1}$.
2. Compute the covariance matrix $\widehat{\boldsymbol{R}}_{\boldsymbol{xx}}$eigenvlaues decomposition (EVD)
$$\widehat{\boldsymbol{R}}_{\boldsymbol{xx}} = \boldsymbol{U\Lambda U}^H \quad (5)$$
Where $\boldsymbol{U}$ is formed by the M orthonormal eigenvalues of $\widehat{\boldsymbol{R}}_{\boldsymbol{xx}}$, and $\boldsymbol{\Lambda}$ is a diagonal matrix containing the corresponding eigenvalues λ_k listed in order of decreasing magnitude.
3. Estimate the model order P using information criteria rules [55].
4. Evaluate the cost function
$$\Im(f) = \frac{1}{\|\boldsymbol{a}^H(f)\widehat{\boldsymbol{G}}\|_F^2} \quad (6)$$
Where $\|.\|_F$ denotes the Frobenius norm and the column vector $\boldsymbol{a}(f)$ is given by
$$\boldsymbol{a}(f) = \left[1, e^{\frac{j\,2\pi f}{F_S}}, e^{\frac{2j\,2\pi f}{F_S}}, \dots, e^{\frac{(M-1)j\,2\pi f}{F_S}}\right] \quad (7)$$
$\widehat{\boldsymbol{G}}$ is formed by the $M-P$ less significant eigenvalues λ_k spanning the noise subspace [56].
5. Find P largest peaks of $\Im(f)$ to obtain the frequency estimates.
6. **Return** Frequency estimates.

Algorithm 2: ESPRIT algorithm

Require: Signal samples $\boldsymbol{x}[n]$.

1. Compute the covariance matrix estimate $\widehat{\boldsymbol{R}}_{\boldsymbol{xx}} = \frac{1}{G}\sum_{n=0}^{G-1} \boldsymbol{x}[n]\boldsymbol{x}[n]^H$. Where $(.)^H$ refers to Hermitian matrix transpose. Since $\boldsymbol{x}[n]$ has length M and we have N observations of $x[n]$, we can construct a set of $G = N - M + 1$ different subvectors $\{\boldsymbol{x}[n]\}_{n=0}^{G-1}$.
2. Compute the covariance matrix $\widehat{\boldsymbol{R}}_{\boldsymbol{xx}}$eigenvlaues decomposition (EVD)
$$\widehat{\boldsymbol{R}}_{\boldsymbol{xx}} = \boldsymbol{U\Lambda U}^H \quad (8)$$
Where $\boldsymbol{U}$ is formed by the M orthonormal eigenvalues of $\widehat{\boldsymbol{R}}_{\boldsymbol{xx}}$, and $\boldsymbol{\Lambda}$ is a diagonal matrix containing the corresponding eigenvalues λ_k listed in order of decreasing magnitude.
3. Estimate the model order P using information criteria rules [55].
4. Obtain the signal subspace $\widehat{\boldsymbol{S}}$ constituted of eigenvectors associated with the P greatest eigenvalues.
$$\widehat{\boldsymbol{S}}_1 = [\boldsymbol{I}_{M-1} \quad \boldsymbol{0}]\widehat{\boldsymbol{S}}$$
$$\widehat{\boldsymbol{S}}_2 = [\boldsymbol{0} \quad \boldsymbol{I}_{M-1}]\widehat{\boldsymbol{S}} \quad (9)$$
5. Compute the eigendecomposition of $\widehat{\boldsymbol{S}}_{12} = [\widehat{\boldsymbol{S}}_1 \quad \widehat{\boldsymbol{S}}_2]$
$$\widehat{\boldsymbol{S}}_{12} = \boldsymbol{E\Lambda E}^{\mathrm{H}} \quad (10)$$
and partition $\boldsymbol{E}$ into $P \times P$ submatrices
$$\boldsymbol{E} = \begin{bmatrix} \boldsymbol{E}_{11} & \boldsymbol{E}_{12} \\ \boldsymbol{E}_{21} & \boldsymbol{E}_{22} \end{bmatrix} \quad (11)$$
6. Calculate Φ the eigenvalues of
$$\Psi = -\boldsymbol{E}_{12}\boldsymbol{E}_{22}^{-1}$$
7. Frequency estimates
$$\widehat{f}_i = \frac{\angle(\Phi_i)}{2\pi}$$
where $\angle(.)$ corresponds to the phase.
8. **Return** Frequency estimates.

Applications for induction machine faults diagnosis are available in [3], [57-59]. In [59], MUSIC and ESPRIT algorithms, and a zooming method were combined to reduce the computational cost of the spectral estimator. ESPRIT algorithm has been combined with Hilbert transform for broken rotor bars fault detection in [60], [61]. However, the performance of such techniques decreases significantly if the noise level increases.

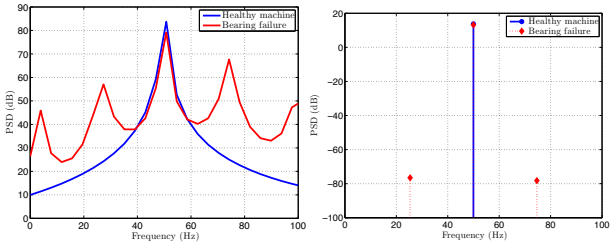

(a) MUSIC-based PSD estimation. (b) RootMUSIC-based PSD estimation.

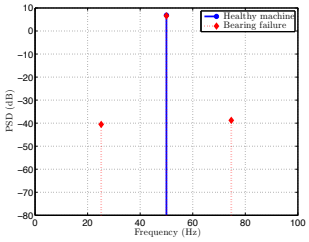

(a) ESPRIT-MLE-based PSD estimation.

Fig. 4. PSD of stator current with bearing fault vs. healthy case using high-resolution techniques.

A maximum likelihood estimation (MLE) approach has been used in [62-63] for mechanical faults (load oscillation and eccentricity faults) and bearing faults detection in induction machine. This technique exploits the faults frequency signature given in the literature to enhance the PSD estimation performance. For mathematical considerations on can refer to [62].

III.2. Non-Stationary Techniques Briefly

The spectral estimation techniques presented earlier are badly suited for inverter driven induction motors, wind turbines and many other applications where the environment is predominantly non-stationary due to transient or variable speed conditions. In non-stationary conditions, fault detection is usually performed by using non-stationary approaches, such as time-frequency or time-scale representations [4], [64]. These approaches include the STFT, the CWT, the WVD and other quadratic distributions, and the HHT. For the sake of clarity, we restrict the presentation here to the discrete-time mathematical formulation. For further details and continuous time equations, the reader could refer to [64]. All the representations, except the last one, have been implemented using the time-frequency toolbox of Matlab [65]. The HHT has been implemented using the G. Rilling's subroutines for Matlab [66].

III.2.1 Spectrogram

The Short-Time Fourier Transform (STFT) is based on the assumption that the signal is quasi-stationary over a short time. It is obtained by computing the Fourier transform for consecutive time frames. It is composed of three steps: first, the signal is divided into time segments, then a time-window $h[.]$ is applied to reduce sidelobe effects and finally, the spectrum of each windowed time frame is computed via the Fourier transform. This procedure, called the STFT, leads to a 3-D representation, which displays the frequency content over time. Let us consider discrete signals of period N. The window $h[n]$ is chosen to be a symmetric discrete signal of period N with norm $\|h\| = 1$. Mathematically, the discrete STFT can be expressed as [67]

$$S_x[m,l] = \sum_{n=0}^{N-1} x[n]h[n-m]\, exp\left(\frac{-j2\pi ln}{N}\right) \qquad (13)$$

For each $0 \le m \le N$, $S_x[m,l]$ is calculated for $0 \le l \le N$ with N FFT procedures of size N. The STFT is a linear transform i.e. $S_{x+y}[m,l] = S_x[m,l] + S_y[m,l]$. The spectrogram is defined as the squared absolute value of the STFT i.e.,$|\, S_x[m,l]|^2$.

Classical choices for $h[n]$ are the rectangular, Hanning, Hamming, or Gaussian window. The length of the window $h[n]$ determines the time and frequency resolution of the representation. This resolution is kept constant over the time-frequency plane, which means that STFT is a mono-resolution technique (Fig. 5(a)). In fact, a short window leads to a representation, which is fine in time but coarse in the frequency domain. Conversely, a long window leads to a representation, which is coarse in time but fine in the frequency domain regardless of the frequency range. This trade-off is formalized by the Heisenberg-Gabor uncertainty space [64]. Figure 6 gives the spectrogram of the stator current in the case of healthy and faulty induction machine. It appears from these figures that, in the presence of the fault, additional frequency components are present and the time-frequency representation allow to track these components over the time and possibly track the fault severity.

The STFT has been investigated for broken bars and bearing faults in [68]. Detection of rotor faults in brushless DC motors has been performed using fault frequencies estimation based on STFT in [69]. In [26], [70], the STFT performance has been compared with the DWT for broken rotor bars and shorted turns with increasing load torque. In [10], the STFT of electromagnetic torque estimation of driving induction machine has been used as a mean of mechanical torsional stresses monitoring.

III.2.2 Scalogram

The Discrete Wavelet Transform (DWT) is obtained by breaking up the signal into shifted and scaled versions of a mother wavelet. Mathematically, the discrete wavelet transform can be expressed as [67]

$$T_x[n,a^l] = \sum_{m=0}^{N-1} x[m]\, \xi_l^*[m-n] \qquad (14)$$

where $(.)^*$ denotes the complex conjugate, a^l is the scale, and $\xi_l[n]$ is the mother wavelet. A discrete wavelet scaled by a^l is defined by

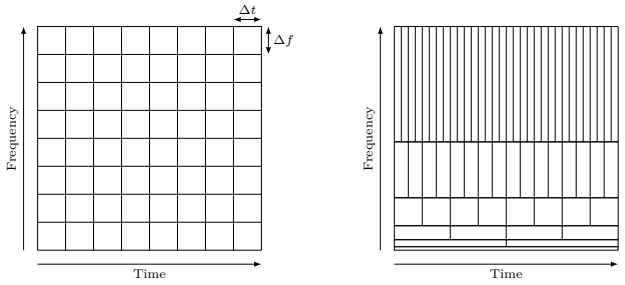

(a) Mono-resolution approach (STFT) (b) Multi-resolution approach (DWT).

Fig. 5. Time-frequency resolution.

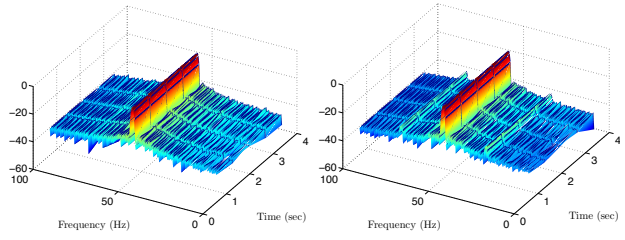

(a) Healty induction machine. (b) Faulty induction machine.

Fig. 6. STFT modulus.

$$\xi_l[n] = \frac{1}{\sqrt{a^l}}\xi\left(\frac{n}{a^l}\right) \quad (15)$$

The DWT is a linear transform i.e. $T_{x+y}[n, a^l] = T_x[n, a^l] + T_y[n, a^l]$. The scalogram is defined as squared absolute value of the DWT i.e., $|T_x[n, a^l]|^2$.

A classical choice for $\xi_l[n]$ is the Mexican-Hat, Morlet or Daubechies wavelets. Rigorously speaking, the DWT leads to a time-scale representation since it displays the signal time evolution at different scales. However, there is a direct link between scale and frequency. Indeed, if the central frequency of the mother wavelet $\xi_l[n]$ is f_0, the scale a^l focuses on the frequency content at $f = \frac{f_0}{a^l}$. As opposed to the STFT, the DWT is a multi-resolution technique, which favors the time-resolution at high frequencies and the frequency resolution at low frequencies (Fig. 5(b)). Unfortunately, the wavelet transform is also limited by the Heisenberg-Gabor principle. Figure 7 gives the stator current scalogram in the case of healthy and faulty machine. The same conclusion can be drawn as in the case of the spectrogram. The main advantage for the scalogram is high resolution when the fault frequency signature is in the high frequency range.

The Continuous wavelet transform (CWT) has been widely investigated for electrical machines monitoring based on the stator current [71]. Detection of dynamic eccentricity in brushless direct current (BLDC) motors operating under dynamic operating conditions has been performed in [72]. In [11], the CWT-based adaptive filter has been used to track the energy in the prescribed time-varying fault-related frequency bands in the power signal in order to perform a cost-effective diagnosis for wind turbines application. The analysis of current transient in induction machine has been employed in [73] using the CWT and B-splines for broken rotor bars fault detection.

III.2.3 Wigner-Ville and other quadratic distributions

As opposed to the previous techniques, which focus on the decomposition of the signal itself, the WVD focuses on the decomposition of the signal energy in the time-frequency plane. Mathematically, the WVD of discrete signal $x[n]$ can be expressed as [67]

$$W_{x,x}[n, k] = \sum_{p=-N}^{N-1} x\left[n + \frac{p}{2}\right] x^*\left[n - \frac{p}{2}\right] exp\left(\frac{-j2\pi kp}{N}\right) \quad (16)$$

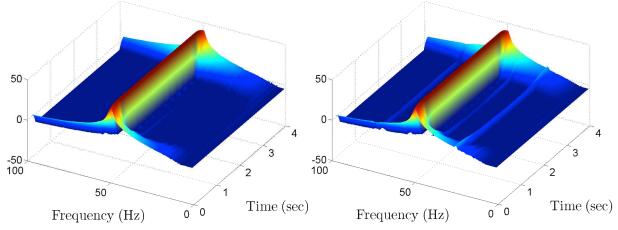

(a) Healty induction machine. (b) Faulty induction machine.

Fig. 7. CWT modulus.

The time-frequency resolution of WVD is not constrained by the Heisenberg Gabor inequality. However, the WVD is non-linear since $W_{(x+y),(x+y)}[n, k] \neq W_{x,x}[n, k] + W_{y,y}[n, k]$. This non-linearity is responsible for the introduction of interference terms. These interference terms can make the time-frequency representation difficult to interpret and may lead to misleading interpretations. To reduce interference terms, the analytic signal is usually employed instead of the signal itself. Furthermore, several authors have proposed extensions of the WVD for interference reduction at the expense of reduced resolution. These extensions have been unified by the Cohen's class of time-frequency distributions [74]. The Cohen's class includes many commonly used time-frequency distributions such as the Pseudo Wigner-Ville, the Choi-Williams, and the Zhao-Atlas-Marks Distributions [75]. The Wigner-Ville distribution exhibits good time and frequency resolution, but it introduces some artifacts in the signal time-frequency representation. In order to remove these cross-terms, a smoothed version of the Wigner-Ville distribution has been proposed. Figure 8 gives the Smoothed Pseudo Wigner-Ville distribution with Hanning smoothing window.

In [14], [51], the authors have proposed the WVD and its extensions in order to perform a time-frequency representation which allows to distinguish load oscillation from eccentricity fault in variable speed induction motors. In [76], the Zhao-Atlas Marks distribution has been used to enhance non-stationary fault diagnostics in electric motors. In [69], the broken rotor bars fault in Brushless DC motors operating under non-stationary conditions has been investigated using the WVD. The short-circuit detection in permanent magnet synchronous motor (PMSM) have been performed using WVD in [77] in the case of steady-state conditions and speed transients.

III.2.4 Hilbert-Huang transform

The Hilbert-Huang Transform (HTT) is the extension of the Hilbert transform for multi-component signals (sum of modulated sine waves). This technique is composed of 2 steps: *i)* first, the signal is decomposed into a sum of amplitude- and frequency modulated mono-component sine waves using an Empirical Mode Decomposition, and then *ii)* the instantaneous amplitude and frequency are extracted using a demodulation technique [78] usually the Hilbert transform. Finally the time-frequency representation is obtained by displaying the time evolution of the instantaneous amplitude and frequency for each sine wave.

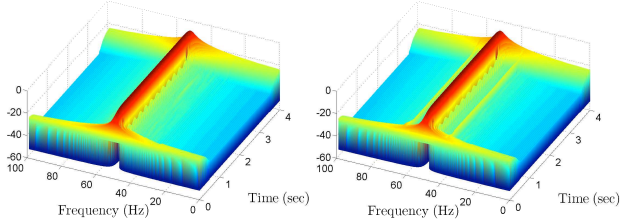

(a) Healty induction machine. (b) Faulty induction machine.

Fig. 8. WVD distribution.

– Empirical mode decomposition (EMD):

The EMD has been originally proposed by Huang [79]. As opposed to the previous techniques, the EMD is essentially defined by an algorithm and does not admit an analytical definition [66]. The algorithm is described by the following steps [79]:

- ✓ Identification of all extrema of $x[n]$.
- ✓ Interpolation between minima (resp. maxima) ending up with some envelope $e_{min}[n]$ (resp. $e_{max}[n]$ [n]).
- ✓ Computation of the mean:

$$m[n] = \frac{e_{min}[n] + e_{max}[n]}{2} \quad (17)$$

- ✓ Extraction of the detail:

✓

$$d[n] = x[n] - m[n] \quad (18)$$

- ✓ Iteration on the residual $m[n]$.

In practice, this algorithm has to be refined by a shifting process until $d[n]$ can be considered as zero-mean. After this procedure, the detail $d[n]$ corresponds to an amplitude- and frequency- modulated (AM/FM) sine wave called Intrinsic Mode Function (IMF). By iterating the algorithm on the residual $m[n]$, the EMD extracts several IMFs until a stopping criterion is reached.

– Instantaneous amplitude (IA) and frequency (IF) extraction:

The IA and IF of each IMF can be extracted using demodulation techniques. To achieve this task, the Hilbert transform is used. In this case the transformation is called, the HHT.

Finally, the time-frequency representation is obtained by displaying the evolution of IA and IF for each IMF in the time-frequency plane. In order to illustrate the performance of the HHT, Fig. 9 gives the time-frequency representation of the stator current. It seems that when the fault occurs the stator current is frequency modulated. The modulation frequency is less than the fundamental frequency. This result is in accordance whit the results presented in [42-43]. In fact, the sidebands around the supply frequency are the proof that the stator currents are frequency or amplitude modulated depending on the defected component of the bearing.

The EMD has been used in [77] to extract IMFs for the actual signal and associated with WVD for PMSM fault detection.

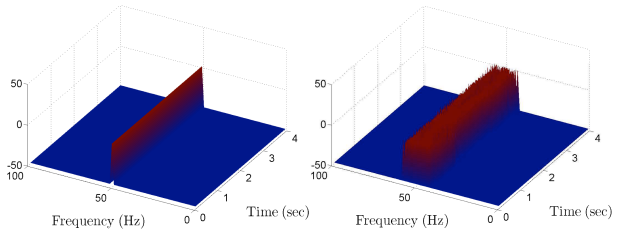

(a) Healty induction machine. (b) Faulty induction machine.

Fig.9. Hilbert Huang transform.

The HHT has been applied to the stator startup current to diagnose the presence of rotor asymmetries in induction machines in [80]. The demagnetization fault in PMSM is analyzed by means of decomposition of stator currents obtained at different speeds using HHT in [81].

IV. Conclusion

This paper has reviewed the induction machine fault detection and diagnosis techniques through a stator currents processing. Attempts have been made to highlight current trends (high resolution techniques, time-frequency/time-scale approaches, etc.). An accurate choice of signal processing techniques for fault detection for several induction machine operating conditions is a key issue. In fact, in transient or in variable speed and/or load, a short data acquisition time is required.

Then, a reliable and efficient technique must be chosen in order to compute an indicator directly related to the fault severity or to stating its occurrence. However, despite of the rich literature, the choice of a particular representation is not an easy task since several parameters must be taken into account.

Using these techniques, additional post-processing algorithms are required to determine the fault-related frequencies and to extract a fault detection criterion. In fact, once the frequency spectrum is computed, empirical algorithms are used in order to reveal frequency signatures in the spectrum within various frequency ranges depending on the failure to be diagnosed. If predicted frequency patterns are present in the spectrum, a positive diagnosis is returned.

In addition to that, to perform induction machine faults diagnosis, a further step is required to achieve a reliable and efficient diagnosis. The artificial intelligence (AI) techniques have been proposed as useful tools to improve the diagnosis, mainly during the decision process. The AI techniques include several sophisticated approaches such as artificial neural networks, support vector machine, Fuzzy logic and many others.

References

[1] M. E. H. Benbouzid, “A review of induction motors signature analysis as a medium for faults detection,” *IEEE Trans. Industrial Electronics*, vol. 47, n°5, pp. 984–993, October 2000.

[2] S. Nandi, H. A. Toliyat, and X. Li, “Condition monitoring and fault diagnosis of electrical motors - A review,” *IEEE Trans. Energy Conversion,* vol. 20, n°4, pp. 719–729, December 2005.

[3] A. Garcia-Perez, R. de Jesus Romero-Troncoso, E. Cabal-Yepez, and R. Osornio-Rios, “The application of high-resolution spectral analysis for identifying multiple combined faults in induction motors,” *IEEE Trans. Industrial Electronics,* vol. 58, n°5, pp. 2002–2010, May 2011.

[4] V. Ghorbanian and J. Faiz, “A survey on time and frequency characteristics of induction motors with broken rotor bars in line-start and inverter-fed modes,” *Mechanical Systems and Signal Processing*, vol. 54-55, pp. 427–456, March 2015.

[5] S. Choi, E. Pazouki, J. Baek, and H. Bahrami, “Iterative condition monitoring and fault diagnosis scheme of electric motor for harsh industrial application,” *IEEE Trans. Industrial Electronics,* vol. 62, n°3, pp. 1760–1769, March 2015.

[6] A. Giantomassi, F. Ferracuti, S. Iarlori, G. Ippoliti, and S. Longhi, "Electric motor fault detection and diagnosis by kernel density estimation and kullback-leibler divergence based on stator current measurements," *IEEE Trans. Industrial Electronics*, vol. 62, n°3, pp. 1770–1780, March 2015.

[7] M. Rausand and A. Hoyland, *System Reliability Theory* (Hoboken: John Wiley & Sons, ISBN 0-471-47133-X, 2004).

[8] L. Meng, J. Xiang, Y. Wang, Y. Jiang, and H. Gao, "A hybrid fault diagnosis method using morphological filter–translation invariant wavelet and improved ensemble empirical mode decomposition," *Mechanical Systems and Signal Processing,* vol. 50, pp. 101–115, 2015.

[9] J. Seshadrinath, B. Singh, and B. K. Panigrahi, "Vibration analysis based interturn fault diagnosis in induction machines," *IEEE Trans. Informatics,* vol. 10, n°1, pp. 340–350, February 2014.

[10] S. Kia, H. Henao, and G. Capolino, "Torsional vibration assessment using induction machine electromagnetic torque estimation," *IEEE Trans. Industrial Electronics,* vol. 57, n°1, pp. 209–219, January 2010.

[11] W. Yang, P. Tavner, C. Crabtreee, and M. Wilkinson, "Cost effective condition monitoring for wind turbines," *IEEE Trans. Industrial Electronics,* vol. 57, n°1, pp. 263–271, January 2010.

[12] J.R. Stack, *Fault signature detection for rolling element bearings in electric machines*, PhD Dissertation, Georgia Institute of Technology, 2002.

[13] J. Ribrant and L. Bertling, "Survey of failures in wind power systems with focus on swedish wind power plant during 1997-2005," *IEEE Trans. Energy Conversion,* vol. 22, n°1, pp. 167–173, March 2007.

[14] M. Blodt, J. Regnier, and J. Faucher, "Distinguishing load torque oscillations and eccentricity faults in induction motors using stator current Wigner distributions," *IEEE Trans. Industry Applications,* vol. 45, no. 6, pp. 1991–2000, November/December 2009.

[15] W. Yang, P. Tavner, and M. Wilkinson, "Wind turbine condition monitoring and fault diagnosis using both mechanical and electrical signatures," *in Proceedings of the 2008 IEEE International Conference on Advanced Intelligent Mechatronics*, Sch. of Mech., Northwestern Polytech. Univ., Xian, Jul. 2008, pp. 1296–1301.

[16] I. S. for petroleum and C. Industry, "Severe duty totally enclosed fan cooled (iefc) squirrel cage induction motors - up to and including 370 kW," *IEEE Std* 841-2001, Tech. Rep., 2001.

[17] B. Maru and P. A. Zotos, "Anti-friction bearing temperature rise for nema frame motors," *IEEE Trans. Industry Applications,* vol. 25, n°5, pp. 883–888, September/October 1989.

[18] Q. Wang, Z. Zhu, J. Duanmu, and X. Ge, "Oil filter debris analysis of aeroengine," *in Proceedings of the 2011 International Conference on Reliability, Maintainability and Safety*, June 2011, pp. 276–278.

[19] M. W. Hawman and W. S. Galinaitis, "Acoustic emission monitoring of rolling element bearings," *in IEEE Proceedings of Ultrasonics Symposium*, October 1988, pp. 885–889.

[20] H. Henao, C. Demian, and G. Capolino, "A frequency-domain detection of stator windings faults in induction machines using an external flux sensor," *IEEE Trans. Industrial Applications*, vol. 39, n°5, pp. 1272–1279, September/October 2003.

[21] E. Elbouchikhi, V. Choqueuse, M. E. H. Benbouzid, and J. F. Charpentier, "Induction machine bearing failures detection using stator current frequency spectral subtraction," *in Proceedings of the 2012 IEEE ISIE*, Hangzhou (China), May 2012, pp. 1228–1233.

[22] E. Elbouchikhi, V. Choqueuse, M. E. H. Benbouzid, J. F. Charpentier, and G. Barakat, "A comparative study of time-frequency representations for fault detection in wind turbine," *in Proceedings of the 2011 IEEE IECON*, Melbourne (Australia), November 2011, pp. 3584–3589.

[23] Y. Amirat, V. Choqueuse, M. E. H. Benbouzid, and S. Turri, "Hilbert transform-based bearing failure detection in DFIG-based wind turbines," *International Review of Electrical Engineering,* vol. 6, n°3, pp. 1249–1256, June 2011.

[24] V. Choqueuse, M. E. H. Benbouzid, Y. Amirat, and S. Turri, "Diagnosis of three-phase electrical machines using multidimensional demodulation techniques," *IEEE Trans Industrial Electronics*, vol. 59, n°4, pp. 2014–2023, April 2011.

[25] S. Watson, B. Xiang, W. Yang, P. Tavner, and C. Crabtree, "Condition monitoring of the power output of wind turbine generators using wavelets," *IEEE Trans. Energy Conversion,* vol. 25, n°3, pp. 715–721, September 2010.

[26] J. Cusido, L. Romeral, J. Ortega, J. Rosero, and A. Espinosa, "Fault detection in induction machines using power spectral density in wavelet decomposition," *IEEE Trans. Industrial Electronics,* vol. 55, n°2, pp. 633–643, February 2008.

[27] M. Blödt, *Condition monitoring of mechanical faults in variable speed induction motor drives, applications of stator current time-frequency analysis and parameter estimation*, PhD Dissertation, INPT, Toulouse, 2006.

[28] A. Bellini, F. Filippetti, C. Tassoni, and G. A. Capolino, "Advances in diagnostic techniques for induction machines," *IEEE Trans. Industrial Electronics,* vol. 55, n°12, pp. 4109–4126, December 2008.

[29] M. Y. Kaikaa and M. Hadjami, "Effects of the simultaneous presence of static eccentricity and broken rotor bars on the stator current of induction machine," *IEEE Trans. Industrial Electronics,* vol. 61, n°5, pp. 2452–2463, June 2014.

[30] B. Liang, S. Iwnicki, and Y. Zhao, "Application of power spectrum, cepstrum, higher order spectrum and neural network analysis for induction motor fault diagnosis," *Mechanical Systems and Signal Processing,* vol. 39, n°1, pp. 342–360, 2013.

[31] F. Duan and R. Zivanovic, "Condition monitoring of an induction motor stator windings via global optimization based on the hyperbolic cross points," *IEEE Trans. Industrial Electronics,* vol. 62, n°3, pp. 1826–1834, March 2015.

[32] A. da Silva, R. Povinelli, and N. Demerdash, "Induction machine broken bar and stator short-circuit fault diagnostics based on three-phase stator current envelopes," *IEEE Trans. Industrial Electronics,* vol. 55, n°3, pp. 1310–1318, March 2008.

[33] P. Shi, Z. Chen, Y. Vagapov, and Z. Zouaoui, "A new diagnosis of broken rotor bar fault extent in three phase squirrel cage induction motor," *Mechanical Systems and Signal Processing,* vol. 42, n°1, pp. 388– 403, 2014.

[34] B. M. Ebrahimi, J. Faiz, S. Lotfi-Fard, and P. Pillay, "Novel indices for broken rotor bars fault diagnosis in induction motors using wavelet transform," *Mechanical Systems and Signal Processing,* vol. 30, pp. 131–145, July 2012.

[35] A. Bellini, F. Filippetti, G. Franceschini, C. Tassoni, and G. B. Kliman, "Quantitative evaluation of induction motor broken bars by means of electrical signature analysis," *IEEE Trans. Industrial Applications,* vol. 37, n°5, pp. 1248–1255, September/October 2001.

[36] M. R. Mehrjou, N. Mariun, M. H. Marhaban, and N. Misron, "Rotor fault condition monitoring techniques for squirrel-cage induction machine–A review," *Mechanical Systems and Signal Processing*, vol. 25, n°8, pp. 2827–2848, November 2011.

[37] B. Ayhan, M. Y. Chow, and M. H. Song, "Multiple discriminant analysis and neural-network-based monolith and partition fault-detection schemes for broken rotor bar in induction motors," *IEEE Trans. Industrial Electronics,* vol. 53, n°4, pp. 1298–1308, June 2006.

[38] G. Didier, E. Ternisien, O. Caspary, and H. Razik, "Fault detection of broken rotor bars in induction motor using a global fault index," *IEEE Trans. Industry Applications,* vol. 42, n°1, pp. 79–88, January/February 2006.

[39] W. He, Y. Zi, B. Chen, F. Wu, and Z. He, "Automatic fault feature extraction of mechanical anomaly on induction motor bearing using ensemble super-wavelet transform," *Mechanical Systems and Signal Processing,* vol. 54-55, pp. 457–480, March 2015.

[40] V. Leite, J. Borges da Silva, G. Veloso, L. da Silva, G. Lambert-Torres, E. Bonaldi, and L. de Oliveira, "Detection of localized bearing faults in induction machines by spectral kurtosis and envelope analysis of stator current," *IEEE Trans. Industrial Electronics*, vol. 62, n°3, pp. 1855–1865, March 2015.

[41] A. Knight and S. Bertani, "Mechanical fault detection in a medium-sized induction motor using stator current monitoring," *IEEE Trans. Energy Conversion,* vol. 29, n°4, pp. 753–760, December 2005.

[42] R. Schoen, T. Habetler, F. Kamran, and R. Bartheld, "Motor bearing damage detection using stator current monitoring," *IEEE Trans. Industry Applications,* vol. 31, n°6, pp. 1274–1279, November/December 1995.

[43] M. Blodt, P. Granjon, B. Raison, and G. Rostaing, "Models for bearing damage detection in induction motors using stator monitoring," *IEEE Trans. Industrial Electronics,* vol. 55, n°4, pp. 1813–1822, April 2008.

[44] E. Elbouchikhi, V. Choqueuse, and M. E. H. Benbouzid, "Current frequency spectral subtraction and its contribution to induction machines' bearings condition monitoring," *IEEE Trans. Energy Conversion*, vol. 28, n°1, pp. 135–144, March 2013.

[45] J. R. Stack, T. G. Habetler, and R. G. Harley, "Fault-signature modeling and detection of inner-race bearing faults," *IEEE Trans. on Industry Applications,* vol. 42, n°1, pp. 61–68, January/February 2006.

[46] J. R. Stack, R. G. Harley, and T. G. Habetler, "An amplitude modulation detector for fault diagnosis in rolling element bearings," *IEEE Trans. Industrial Electronics,* vol. 51, n°5, pp. 1097–1102, October 2004.

[47] E. Fournier, A. Picot, J. Regnier, P. Maussion, J. Andrejak, and M. Tientcheuyamdeu, "Current-based detection of mechanical unbalance in an induction machine using spectral kurtosis with reference," *IEEE Trans. Industrial Electronics,* vol. 62, n°3, pp. 1879–1887, March 2015.

[48] J. Faiz, B. M. Ebrahimi, B. Akin, and H. A. Toliyat, "Finite-element transient analysis of induction motors under mixed eccentricity fault," *IEEE Trans. Magnetics,* vol. 44, n°1, pp. 66–74, January 2008.

[49] G. M. Joksimovic, "Dynamic simulation of cage induction machine with air gap eccentricity," *IEE Proc – Electric Power Applications*, vol. 152, n°4, pp. 803–811, July 2005,

[50] B. Heller and V. Hamata, *Harmonic Field Effects in Induction Machine* (Elsevier Scientific Publishing Company, 1977).

[51] M. Blodt, D. Bonacci, J. Regnier, M. Chabert, and J. Faucher, "Online monitoring of mechanical faults in variable-speed induction motor drives using the Wigner distribution," *IEEE Trans. Industrial Electronics*, vol. 55, n°2, pp. 522–533, February 2008.

[52] S. Kay, *Modern Spectral Estimation: Theory and Application (*Prentice Hall, Englewood Cliffs, New Jersey, 1998).

[53] S. Kay and S. Marple, "Spectrum analysis - a modern perspective," *Proceedings of the IEEE,* vol. 69, n°11, pp. 1380–1419, November 1981.

[54] P. Stoica and R. L. Moses, *Introduction to Spectral Analysis* (Prentice- Hall,New Jersey, 1997).

[55] P. Stoica and Y. Selen, "A review of information criterion rules," *IEEE Signal Processing Magazine*, vol. 21, n°4, pp. 36–47, July 2004.

[56] P. Stoica and A. Nehorai, "MUSIC, maximum likelihood, and Cramer-Rao bound," *IEEE Trans. Acoustics, Speech and Signal Processing*, vol. 37, n°5, pp. 720–741, May 1989.

[57] F. Cupertino, E. de Vanna, L. Salvatore, and S. Stasi, "Analysis techniques for detection of im broken rotor bars after supply disconnection," *IEEE Trans. Industry Applications*, vol. 40, n°2, pp. 526–533, March/April 2004.

[58] A. Bracale, G. Carpinelli, L. Piegari, and P. Tricoli, "A high resolution method for on line diagnosis of induction motors faults*," in Proceedings of 2007 IEEE PowerTech*, Lausanne, (Switzerland), July 2007, pp. 994–998.

[59] S. H. Kia, H. Henao, and G. A. Capolino, "A high-resolution frequency estimation method for three-phase induction machine fault detection*," IEEE Trans. Industrial Electronics,* vol. 54, n°4, pp. 2305–2314, August 2007.

[60] B. Xu, L. Sun, L. Xu, and G. Xu, "Improvement of the Hilbert method via ESPRIT for detecting rotor fault in induction motors at low slip," *IEEE Trans. Energy Conversion,* vol. 28, n°1, pp. 225–233, March 2013

[61] Y. Kim, Y.and Youn, Hwang, D. Sun, and D. J.; Kang, "High-resolution parameter estimation method to identify broken rotor bar faults in induction motors," *IEEE Trans. Industrial Electronics*, vol. 60, n°9, pp. 4103–4117, November 2013.

[62] E. Elbouchikhi, V. Choqueuse, and M. Benbouzid, "Induction machine faults detection using stator current parametric spectral estimation," *Mechanical Systems and Signal Processing*, vol. 52-53, pp. 447–464, February 2015.

[63] M. Blodt, M. Chabert, J. Regnier, and J. Faucher, "Current based mechanical fault detection in induction motors through maximum likelihood estimation," *in Proceedings of the 2006 IEEE IECON*, Paris (France), November 2006, pp. 4999–5004.

[64] P. Flandrin, *Time-frequency/time-scale analysis* (Academic Press, 1998).

[65] F. Auger, P. Flandrin, P. Goncalves, and O. Lemoine, "Time-frequency toolbox, for use with Matlab," CNRS, GDR ISIS, Tech. Rep., 1997.

[66] G. Rilling, P. Flandrin, and P. Gonalves, "On empirical mode decompositionand its algorithms," *in Proceedings of the 2003 IEEE-EURASIP Workshop on Nonlinear Signal and Image Processing*, Grado (Italia), 2003.

[67] S. Mallat, *A Wavelet Tour of Signal Processing: The Sparse Way* (3rd ed. Academic Press, 2008).

[68] B. Yazici and G. Kliman, "An adaptive statistical time-frequency method for detection of broken bars and bearing faults in motors using stator current," *IEEE Trans. Industry Applications,* vol. 35, n°2, pp. 442–452, March/April 1999.

[69] S. Rajagopalan, J. Aller, J. A. Restrepo, T. Habetler, and R. Harley, "Detection of rotor faults in brushless dc motors operating under nonstationary conditions*," IEEE Trans. Industry Applications,* vol. 42, n°6, pp. 1464 – 1477, November/December 2006.

[70] E. Cabal-Yepez, A. G. Garcia-Ramirez, R. J. Romero-Troncoso, A. Garcia-Perez, and R. A. Osornio-Rios, "Reconfigurable monitoring system for time-frequency analysis on industrial equipment through STFT and DWT," *IEEE Trans. Industrial Informatics*, vol. 9, n°2, pp. 760–771, May 2013.

[71] H. Sun, Z. He, Y. Zi, J. Yuan, X. Wang, J. Chen, and S. He, "Multiwavelet transform and its applications in mechanical fault diagnosis–A review," *Mechanical Systems and Signal Processing*, vol. 43, n°1, pp. 1–24, 2014.

[72] S. Rajagopalan, J. Aller, J. A. Restrepo, T. Habetler, and R. Harley, "Analytical-wavelet-ridge-based detection of dynamic eccentricity in brushless direct current (BLDC) motors functioning under dynamic operating conditions," *IEEE Trans. Industrial Electronics*, vol. 54, n°3, pp. 1410–1419, june 2007.

[73] J.Pons-Llinares, J. Antonino-Daviu, M. Riera-Guasp, M. Pineda-Sanchez, and V. Climente-Alarcon, "Induction motor diagnosis based on a transient current analytic wavelet transform via frequency b-splines," *IEEE Trans. Industrial Electronics*, vol. 58, n°5, pp. 1530–1544, May 2011.

[74] L. Cohen, "*Time-frequency distributions-a review*," Proceedings of the IEEE, vol. 77, n°7, pp. 941–981, July 1989.

[75] F. Auger and P. Flandrin, "Improving the readability of time-frequency and time-scale representations by the reassignment method," *IEEE Trans. Signal Processing*, vol. 43, n°5, pp. 1068–1089, May 1995.

[76] S. Rajagopalan, J. A. Restrepo, J. Aller, T. Habetler, and R. Harley, "Nonstationary motor fault detection using recent quadratic time-frequency representations," *IEEE Trans. Industry Applications*, vol. 44, n°3, pp. 735–744May/June 2008.

[77] J. Rosero, L. Romeral, J. Ortega, and E. Rosero, "Short-circuit detection by means of empirical mode decomposition and Wigner-Ville distribution for PMSM running under dynamic condition," *IEEE Trans. Industrial Electronics*, vol. 56, n°11, pp. 4534–4547, November 2009.

[78] E. Elbouchikhi, V. Choqueuse, M. Benbouzid, and J. A. Antonino-Daviu, "Stator current demodulation for induction machine rotor faults diagnosis," *in Proceedings of the 2014 IEEE ICGE*, Sfax (Tunisia), March 2014, pp. 176–181.

[79] N. Huang, Z. Shen, S. Long, M. Wu, H. Shih, Q. Zheng, N. Yen, C. Tung, and H. Liu, "The empirical mode decomposition and Hilbert spectrum for nonlinear and nonstationary time series analysis," *Proc., Roy. Soc. London*, vol. 454, pp. 903–995, 1998.

[80] J. Antonino-Daviu, M. Riera-Guasp, M. Pineda-Sanchez, and R. Prez, "A critical comparison between DWT and Hilbert-Huang-based methods for the diagnosis of rotor bar failures in induction machines," *IEEE Trans. Industry Applications*, vol. 45, n°5, pp. 1794–1803, September/October 2009.

[81] A. Espinosa, J. Rosero, J. Cusido, L. Romeral, and J. Ortega, "Fault detection by means of Hilbert-Huang transform of the stator current in a PMSM with demagnetization," *IEEE Trans. Energy Conversion*, vol. 25, n°2, pp. 312–318, June 2010.

[1]ISEN Brest, EA 4325 LBMS, 20, Rue Cuirassé Bretagne, 29200 Brest, France (email: elbouchikhi@isen-bretagne.fr).
[2]University of Brest, EA 4325 LBMS, Rue de Kergoat, CS 93837, 29238 Brest Cedex 03, France (e-mail: Vincent.Choqueuse@univ-brest.fr, Mohamed.Benbouzid@univ-brest.fr).
[3]Shanghai Maritime University, 201306 Shanghai, China

Elhoussin Elbouchikhi was born in Khemisset, Morocco, in 1987. He received the diploma engineer degree (Dipl.-Ing.) in Automatic and Electrical Engineering and Research Master's degree in Automatic Systems, Computer Science and Decision, from the National Polytechnic Institute of Toulouse (ENSEEIHT), Toulouse, France, in 2010, and the Ph.D degree in 2013 from the University of Brest, Brest, France. He has been a Post-Doctoral Researcher at ISEN Brest, Brest, France and an Associate Member of the *LBMS_Lab* (EA 4325) from October 2013 to September 2014. Since September 2014, he is an Associate Professor at ISEN Brest, Brest, France and an affiliated member of the *LBMS_Lab* (EA 4325).

His current research interests include electrical machines faults detection and diagnosis, and signal processing and statistics for power systems monitoring.

Vincent Choqueuse was born in Brest, France, in 1981. He received the Dipl.-Ing. and the M.Sc. degrees in 2004 and 2005, respectively, from the Troyes University of Technology, Troyes, France, and the PhD degree in 2008 from the University of Brest, Brest, France. Since September 2009, he has been an Associate Professor with the Institut Universitaire de Technologie of Brest, University of Brest, Brest, France, and a member of the Mechanics and Systems Laboratory of Brest (*LBMS_Lab*, EA 4325).

Dr. Choqueuse research interests include signal processing and statistics for power systems monitoring, Smart-Grid, digital communication and digital audio. He has also developed a free web application for online signal processing and analysis: www.sp4mass.com.

Mohamed El Hachemi Benbouzid was born in Batna, Algeria, in 1968. He received the B.Sc. degree in electrical engineering from the University of Batna, Batna, Algeria, in 1990, the M.Sc. and Ph.D. degrees in electrical and computer engineering from the National Polytechnic Institute of Grenoble, Grenoble, France, in 1991 and 1994, respectively, and the Habilitation à Diriger des Recherches degree from the University of Picardie "Jules Verne," Amiens, France, in 2000.

After receiving the Ph.D. degree, he joined the Professional Institute of Amiens, University of Picardie "Jules Verne," where he was an Associate Professor of electrical and computer engineering. Since September 2004, he has been with the Institut Universitaire de Technologie of Brest, University of Brest, Brest, France, where he is a Professor of electrical engineering. Prof. Benbouzid is also a Distinguished Professor at the Shanghai Maritime University, Shanghai, China. His main research interests and experience include analysis, design, and control of electric machines, variable-speed drives for traction, propulsion, and renewable energy applications, and fault diagnosis of electric machines.

Prof. Benbouzid is an IEEE Senior Member. He is the Editor-in-Chief of the INTERNATIONAL JOURNAL ON ENERGY CONVERSION (IRECON). He is also an Associate Editor of the IEEE TRANSACTIONS ON ENERGY CONVERSION, the IEEE TRANSACTIONS ON INDUSTRIAL ELECTRONICS, the IEEE TRANSACTIONS ON SUSTAINABLE ENERGY, and the IEEE TRANSACTIONS ON VEHICULAR TECHNOLOGY. He was an Associate Editor of the IEEE/ASME TRANSACTIONS ON MECHATRONICS from 2006 to 2009.